Subterahertz Acoustical Pumping of Electronic Charge in a Resonant Tunneling Device

E. S. K. Young, A. V. Akimov, M. Henini, L. Eaves, and A. J. Kent
School of Physics and Astronomy, University of Nottingham, Nottingham NG7 2RD, United Kingdom
(Received 15 December 2011; published 31 May 2012)

We demonstrate that controlled subnanosecond bursts of electronic charge can be transferred through a resonant tunneling diode by successive picosecond acoustic pulses. The effect exploits the nonlinear current-voltage characteristics of the device and its asymmetric response to the compressive and tensile components of the strain pulse. This acoustoelectronic pump opens new possibilities for the control of quantum phenomena in nanostructures.

DOI: 10.1103/PhysRevLett.108.226601 PACS numbers: 72.80.Ey, 72.50.+b, 85.30.Hi

The coupling of dynamical strain to the electrons in nanostructures gives rise to the possibility of probing and control of quantum electronic states using nanoacoustic waves. Currently, there is considerable interest in the interaction of elastic waves, which have frequencies in the range 10^{10}–10^{12} Hz corresponding to wavelengths of micrometer to nanometer range, with electronic and optical nanodevices. Potential applications are anticipated in such fields as microscopy [1,2], ultrafast x ray [3], THz electronics [4] and nanophotonics [5], as well as in the generation, and detection of nanoacoustic waves for realizing ''sound ideas'' concepts [6].

Hypersonic waves generated and detected by femtosecond optical pump-probe techniques are now commonly used to investigate physical phenomena in nanostructures such as quantum dots [7], *p-n* diodes [8], phonon nanocavities [9] and freestanding membranes [10]. Experiments with GHz surface acoustic waves [11,12] and picosecond strain pulses [13] in optical microcavities with quantum wells and quantum dots have shown strong modulation of the light emitted by nanodevices. This has led to the proposal that nanoacoustics could be used to study a broad range of quantum phenomena [14].

The effects of hypersonic waves on the quantum electronic transport properties of nanodevices have received much less attention, and there are outstanding fundamental questions, e.g., relating to the charge transport mechanisms, sensitivity, and speed of response, that must be addressed before applications can be realized. Acoustic control of electron transport in nanodevices, including tunneling devices, has been achieved using surface acoustic waves [15,16]. However, for this technique, the upper frequency is limited to a few GHz by the dimensions of the ultrasonic transducer. New information about the interaction of sub-THz and THz hypersonic waves with current carriers has been obtained by measuring the acoustoelectric response of bulk [17] and junction devices [18], but these methods have limited temporal resolution and sensitivity.

In this Letter we investigate the effect of a hypersonic wave packet on the transport properties of a semiconducting quantum device: a double-barrier resonant tunneling diode (RTD). We detect the time-integrated charge transferred through the barriers of the device due to the passage of a hypersonic wave packet. The response, which is dependent on the nonlinear electrical properties of the device and is thus qualitatively different to the linear response of bulk and junction devices previously studied [17,18], exhibits a very strong sensitivity to dynamical strain and provides subnanosecond time resolution. The basic principle of operation is illustrated in Fig. 1, which shows schematically the band diagram of a RTD with a two-dimensional (2D) electron emitter [19] when the voltage drop between the collector and emitter reservoirs, V_d, corresponds to the threshold (a)

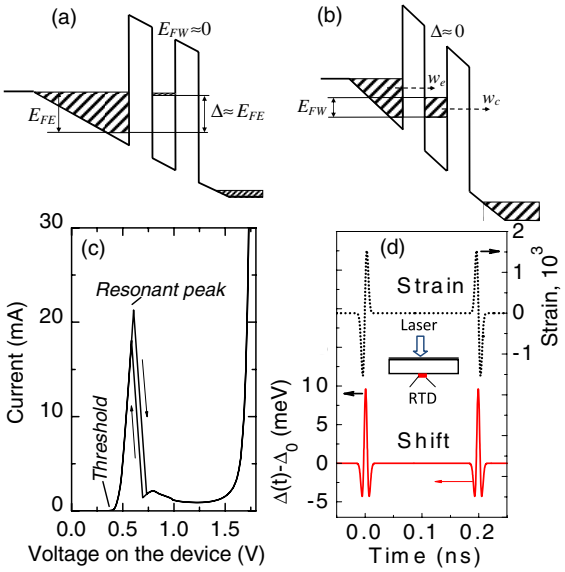

FIG. 1 (color online). Schematic band diagrams of a double-barrier resonance tunneling diode (RTD) biased near the resonant threshold (a) and the resonant peak (b). (c) The current-voltage characteristic of the device measured for increasing and decreasing the bias voltage. (d) Temporal evolutions of the strain in the middle of the first barrier (top, dotted curve) and of the strain-induced shift between the electron levels in the quantum well and the 2D emitter (bottom, solid curve). The experimental setup is shown schematically in the inset in (d).

and peak (b) of the resonance in the current-voltage curve [see Fig. 1(c)]. In semiconductors, acoustoelectrical effects are governed mainly by the strong dependence of the energy of the electron states on dynamical strain, which accompanies the THz acoustic wave packet [20]. Thus the hypersonic wave, which propagates with the longitudinal sound velocity, modulates the energy separation, Δ, between the electron states in the 2D emitter and quantum well (QW) of the RTD. The response to Δ is similar to that to V_d and hence the resonant tunnel current is also modulated by the strain pulse.

The strain-induced modulation leads to a particularly strong asymmetric response of the current to the sign of the dynamical strain-induced shift $\Delta(t) - \Delta_0$, where Δ_0 is the stationary detuning from resonance in the absence of the strain pulse. This asymmetry is most pronounced when the RTD is biased at the threshold at which $\Delta_0 = E_{FE}$, where E_{FE} is the Fermi level in the emitter and also at the peak of the resonance ($\Delta_0 = 0$). Indeed, at the threshold [Fig. 1(a)], the stationary current I_0 is very small, and current starts to flow only if the strain pulse induces the shift of the levels in the emitter and QW towards resonance, i.e., $\Delta(t) - \Delta_0 < 0$. In the opposite case, $\Delta(t) - \Delta_0 > 0$, the electron ground state in the QW moves above the Fermi level in the emitter and, at low temperature, the current is negligible. On the other hand, at the resonant peak [Fig. 1(b)], I_0 is a maximum and values of $\Delta(t) - \Delta_0$ of either sign lead to a marked decrease of I_0, i.e., $\Delta I(t) < 0$. In these two extreme cases, the current integrated over a period of time, which exceeds the duration of the hypersonic wave packet is nonzero. The current response of a RTD to the hypersonic signal is analogous to the working of a mechanical pump, in which a system admits and expels the pumped fluid when the piston is moving in the backwards and forwards directions, respectively.

Our *n-i-n* RTD structure was grown by molecular beam epitaxy (MBE) on a semi-insulating GaAs substrate. It comprises a 5 nm GaAs quantum well between two 5.5 nm wide undoped $Al_{0.4}Ga_{0.6}As$ barriers. The emitter and collector layers consist of 2.5 nm undoped GaAs spacers separating the barriers from 50 nm *n*-doped GaAs layers, in which the doping increases linearly from 5×10^{14} cm^{-3} adjacent to the spacers to 2×10^{16} cm^{-3}. The top and substrate side n^+ contacts consist of 0.5 μm and 3 μm of GaAs (doped at 2×10^{18} cm^{-3}), respectively. The sample was processed into 100 μm cylindrical mesas and InGeAu Ohmic contacts made to the n^+ layers. Detailed electronic transport studies of the same and similar RTD devices [19] showed that at V_d above the threshold, but below the resonant peak, the 2D electron density in the emitter remains constant and has a value $n_e \approx 1.5 \times 10^{11}$ cm^{-2}, corresponding to a Fermi energy $E_{FE} = 15$ meV. In this bias range the quasi-2D subband levels in the emitter and QW are closely aligned. From the (*I-V*) curve shown in Fig. 1(c) we can deduce the Fermi energy in the QW at the peak of the resonance, $E_{FW} = 7.5$ meV, and the electron tunneling time from the QW to the collector: $\tau_c = 200$ ps.

Strain pulses were generated in a 100 nm thick Al film deposited on the back side of the GaAs substrate. The film was excited using 400 nm wavelength, 60 fs duration, optical pump pulses from an amplified titanium-sapphire laser of repetition rate 5 kHz, focused onto a spot of diameter 200 μm directly opposite the device mesa. This excitation generates bipolar strain pulses of duration $\sim$15 ps via thermoelastic effects in the Al film [21]. The strain pulses propagate through the GaAs substrate and pass the RTD twice with an interval $\sim$200 ps: the first time on the way to the sample surface and the second time while moving in the opposite direction after reflection from the surface with a π-phase change. The model simulations of the strain $\varepsilon(t)$ in the middle of the QW with an amplitude $\varepsilon_0 \sim 1.5 \times 10^{-3}$ is shown schematically in Fig. 1(d) by the dotted line. For simplicity, we ignore the nonlinear properties of the strain pulse propagation in the GaAs [22]. Using $\varepsilon(t)$, the speed of longitudinal sound in GaAs ($s_{LA} = 4.8 \times 10^3$ m/s) and the deformation potential $\Xi = -7$ eV [23], we deduce the time-dependent shift $\Delta(t) - \Delta_0$ as shown by the solid line in Fig. 1(d).

The changes in the current, $\Delta I(t) = I(t) - I_0$, induced by the strain modulation of Δ were recorded by a Textronix digital oscilloscope with an analogue bandwidth of 12.5 GHz, and are shown in Fig. 2 for various bias voltages,

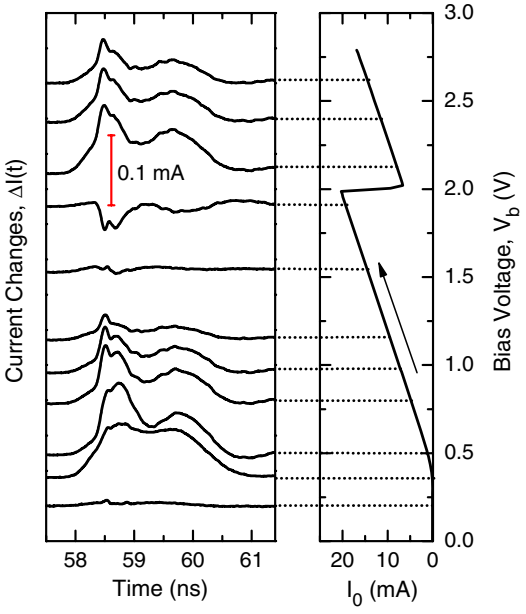

FIG. 2 (color online). The strain-induced current pulses measured at various bias voltages, V_b. The corresponding V_b is shown by the dotted lines connecting the measured current pulses with the corresponding point at the I_0-V_b characteristic presented on the right panel. The time is counted relative to the moment when the pump pulse hits the metal film at the surface opposite to the RTD device.

V_b, applied across the series combination of the device and 50 Ω load resistor. The dependence $I_0(V_b)$ in the right panel of Fig. 2 corresponds to changing V_b in the forward bias direction. The deviation of $\Delta I(t)$ from zero starts when the strain pulse reaches RTD in a time $t_0 = d/s_{\mathrm{LA}} \approx 58$ ns after the pump pulse, where $d = 278$ μm is the distance from the Al transducer to the RTD. The sign of the $\Delta I(t)$ changes from positive to negative when V_b increases from the threshold towards the peak of the resonance, and then $\Delta I(t)$ changes again to positive when the peak is passed. The temporal shape of $\Delta I(t)$ has a two-humped profile and an overall duration ~2 ns, which significantly exceeds the duration of the strain pulse. When V_b is varied in the opposite direction, from $V_b = 3$ V to 0, the dependence of $I_0(V_b)$ differs from that shown in the side panel in Fig. 2 due to the well-known bistability effect in RTDs [24]. This case does not affect the main conclusions of the present Letter and thus will not be considered further here.

Figure 3(a) shows the temporal profiles $\Delta I(t)$ measured for the highest pump power density, $P = 10$ mJ cm^{-2}, on the Al transducer and three values of V_b, increasing sequentially from V_b near the threshold ($V_b = 0.5$ V), through the rising part of the (I-V) curve ($V_b = 1$ V) and on to the peak of the tunneling resonance ($V_b = 1.8$ V). As noted earlier, $\Delta I(t) > 0$ at the threshold and $\Delta I(t) < 0$ near the peak. Between these extreme cases $\Delta I(t) > 0$ but the amplitude is lower than at the threshold. The signal $\Delta I(t)$ shows fine structure over a time interval $t = 58$ to 59 ns which appears as two overlapping peaks with separation 200 ps. This separation is better resolved near the resonant peak than at the threshold.

Of particular interest is the high amplitude of the $\Delta I(t)$ measured. The relative changes of the current are ~10% at the threshold and ~1% at the peak for our highest value of

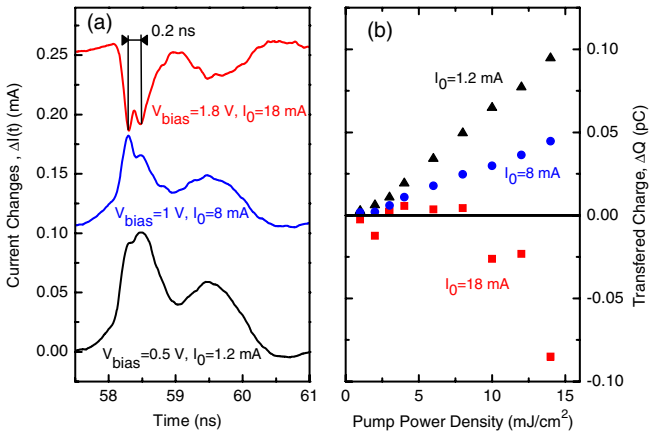

FIG. 3 (color online). (a) Strain-induced current pulses measured at pump density 10 mJ/cm^2 for bias voltages corresponding to the resonant threshold (lower curve), halfway up the resonant peak in (I_0-V_b) (middle curve) and near the peak of the resonance (upper curve). (b) The strain-induced charge transferred through the device due to the action of the strain pulse as a function of pump density. The traces are offset for clarity.

P. The signals are also free from any heat pulse background. Since $\Delta I(t)$ is also dependent on the temporal response of the system, instead of considering the peak change of current, we consider the total charge ΔQ transferred though the RTD as a result of the strain-induced changes in current ΔI: $\Delta Q = \int \Delta I(t) dt$. The dependence of ΔQ on P, shown in Fig. 3(b), is generally nonlinear and depends on V_b. Especially strong nonlinearity is observed for V_b near the peak current ($V_b = 1.8$ V, $I_0 = 18$ mA), when the strain-induced changes $|\Delta Q|$ are not noticeable for $P < 10$ mJ/cm^2 and rapidly increase with increasing P.

These results are a clear experimental demonstration of controlled charge transfer through the RTD during the action of the strain pulse which acts effectively as an acoustic pump. We now quantify our model of the acoustic pumping effect in a RTD by means of a more detailed analysis, which makes use of the phenomenological tunneling rates that follow from a detailed quantum mechanical consideration of the tunneling processes [25]. We include the effects of charge accumulation in the GaAs QW by solving the kinetic equation for E_{FW} at zero temperature ($T = 0$):

$$\frac{dE_{FW}}{dt} = -(w_c + w_e)E_{FW} + [E_{FE} - \Delta(t)]w_e\{H[E_{FE} - \Delta(t)]\}, \quad (1)$$

where $H(x)$ is the Heaviside function. The time-dependent function $\Delta(t)$ includes the sum of stationary detuning, Δ_0, and the strain-induced shift shown in Fig. 1(d) by the solid line. The coefficient w_c is the electron tunneling rate from the QW to the collector, and is independent of Δ. The rate for an electron to tunnel from the emitter to a nonoccupied state in the QW or back from the QW to an available state in the emitter is w_e, and this passes through a resonance when the ground electron states in the emitter and QW are aligned ($\Delta = 0$). Assuming a Lorentzian resonance profile we have:

$$w_e = \frac{w_R \Gamma^2}{\Gamma^2 + \Delta^2(t)}, \quad (2)$$

where w_R is the tunneling rate at resonance and Γ characterizes the resonance damping. In our calculations we use $w_c = w_R = 5 \times 10^9$ s^{-1}, estimated from the dc (I-V_d) curve [Fig. 1(c)] and $\Gamma = 12$ meV.

The values which we deduce for $\Delta I(t) = w_c n_w e S$ are shown in Figs. 4(a) and 4(b) for high and low strain amplitude ε_0, respectively. Here $n_w = m^* E_{FW}/\pi\hbar^2$ is the sheet density of 2D electrons in the QW and S is the device area. The curves in Figs. 4(a) and 4(b) show $\Delta I(t)$ for three values of stationary detuning: at the threshold ($\Delta_0 = E_{FE}$); half way up to the resonant peak ($\Delta_0 = 0.5E_{FE}$); and at the peak of the resonance ($\Delta_0 = 0$).

The main qualitative result of our simulations: the dependence of the sign of the calculated ΔQ on Δ_0, which is directly related to V_b in our experiment, is fully consistent

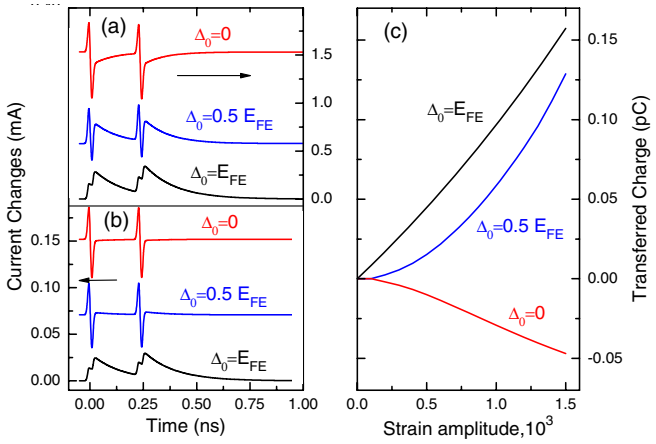

FIG. 4 (color online). Model calculations. Temporal evolutions of the current changes induced by strain pulses with amplitudes $\varepsilon_0 = 10^{-3}$ (a) and $\varepsilon_0 = 10^{-4}$ (b), calculated when the device is biased at the resonant threshold (lower curves), halfway up the resonant peak in the (I-V) curve (middle curves) and at the peak of the resonance (upper curves). The strain pulse arrival time to the RTD is set as $t = 0$. For comparison with experimental results, note the different time scales in (a) and Fig. 3. (c) The strain-induced charge transferred through the RTD during the action of the strain pulse as a function of strain pulse amplitude for various amounts of detuning between electron levels in the QW and emitter.

with our experimental data. Near the threshold ($\Delta_0 \approx E_{FE}$) $\Delta Q > 0$; and at the resonant peak ($\Delta_0 \approx 0$) $\Delta Q < 0$, as observed in experiment. We also obtain good quantitative agreement between the measured and calculated absolute values for ΔQ. The calculations give $|\Delta Q| \sim 0.1$ pC for $\varepsilon_0 \sim 10^{-3}$. In the experiments this value of ε_0 is realized by exciting the Al film on the GaAs with an energy density $P \sim 10$ mJ/cm^2 [26]. Under such conditions we measure a value $|\Delta Q|$ very close to the calculated one [see Fig. 3(b)], thus providing strong support for the validity of the model.

A close comparison of the experimental and calculated temporal shapes of $\Delta I(t)$ in Figs. 3(a) and 4(a) reveals that the fast picosecond features in the calculated curves are not detected in the experimentally measured $\Delta I(t)$. Moreover, the peak, which is delayed by $\sim$1 ns relative to the maximum of the strain-induced current observed in the experiment, is not predicted by the model. We attribute this to the first cycle of a $\sim$1 GHz ringing superimposed on the decaying tail of the signal. The ringing, which is excited by the transient current pulse, is due to the oscillations of a resonant electrical circuit comprised of the RTD capacitance and the parasitic inductance and capacitance of the device packaging [27]. Interestingly, the temporal response at threshold is noticeably slower than at higher V_b, [compare $\Delta I(t)$ curves for various V_b in Fig. 2]. This can be understood in terms of the increase of tunneling rates with increasing V_b on approach to resonance and the decrease of the effective barrier height. Hence the expected 0.2 ns separation between the peaks related to incident and reflected strain pulses is more pronounced in the experimental curves for higher V_b.

The calculated and experimental dependences of ΔQ on strain amplitude ε_0 are in general nonlinear [compare Fig. 4(c) with Fig. 3(b)]. This is because integration of the ε-linear component of $\Delta I(t)$ over the time interval when the strain pulse is passing through the RTD is zero due to the bipolar nature of the strain pulse. The exception is the case when the RTD is biased exactly at the threshold and the rectified response is linear with the time-integrated $\Delta(t)$ [Fig. 1(a)]. The signals $\Delta I(t)$ measured at the threshold appear to have the highest amplitude for all pump excitations [see Fig. 3(b)]. We attribute the weak superlinear behavior for $P < 2$ mJ/cm^2 to the thermal smearing of the electron distribution at $T = 5$ K.

Our experimental data and their agreement with our model calculations demonstrate the high level of control provided by the acoustic pumping technique which for a RTD may be considered as a hypersonic prototype of the detection of an oscillating electric field using a rectifying device. The sensitive detection of the integrated sub-THz acoustic flux by measuring the charge transferred through the device is not inhibited by the relatively limited temporal resolution. This is a particular advantage of the acoustic pumping approach.

In conclusion, we have demonstrated that a picosecond strain pulse induces changes in the current passing through a semiconductor resonant tunneling device. The amount and sign of the integrated charge transferred through the device during the passage of the pulse can be precisely controlled by changing the bias voltage and the strain amplitude. We find that the fraction of electrons in the QW that are transferred though the barrier and into the collector on a subnanosecond time scale is as much as 10% at high strain pulse amplitudes. The effect, which arises from the strong nonlinearity of the current-voltage characteristics, is similar to mechanical pumping of a fluid, where a system of valves is used to prevent backflow. The maximum charge transferred by acoustic pumping is achieved at the threshold for dc resonant tunneling, when the current though RTD starts to flow. The results of model calculations agree with experiment.

Sub-THz acoustic pumping has the potential for future applications in high-frequency acoustics. The technique has high sensitivity to dynamical strain and provides subnanosecond temporal resolution. Thus measuring the charge passing through a tunneling device acts as a sensitive detector of hypersonic signals. The acoustic pumping concept may be also used to control the charge and current in tunneling devices, a feature which may find applications in the integrated sub-THz and THz acoustoelectronic devices.

We acknowledge the support for this work from the Engineering and Physical Sciences Research Council of the UK, and Dr. Boris Glavin for helpful discussions.

[1] H. J. Maris, Sci. Am. **278**, 86 (1998).
[2] K. H. Lin, C. M. Lai, C. C. Pan, J. I. Chyi, J. W. Shi, S. Z. Sun, C. F. Chang, and C. K. Sun, Nature Nanotech. **2**, 704 (2007).
[3] M. Bargheer, N. Zhavoronkov, Y. Gritsai, J. C. Woo, D. S. Kim, M. Woerner, and T. Elsaesser, Science **306**, 1771 (2004).
[4] M. R. Armstrong, E. J. Reed, Ki-Yong Kim, J. H. Glownia, W. M. Howard, E. L. Piner, and J. C. Roberts, Nature Phys. **5**, 285 (2009).
[5] N. D. Lanzillotti-Kimura, A. Fainstein, A. Huynh, B. Perrin, B. Jusserand, A. Miard, and A. Lemaitre, Phys. Rev. Lett. **99**, 217405 (2007).
[6] T. Gorishnyy, M. Maldovan, C. Ullal, and E. L. Thomas, Phys. World **18**, 24 (2005).
[7] A. Devos, F. Poinsotte, J. Groenen, O. Dehaese, N. Bertru, and A. Ponchet, Phys. Rev. Lett. **98**, 207402 (2007).
[8] K.-H. Lin, C.-T. Yu, Y.-C. Wen, and C.-K. Sun, Appl. Phys. Lett. **86**, 093110 (2005).
[9] N. D. Lanzillotti-Kimura, A. Fainstein, A. Lemaitre, B. Jusserand, and B. Perrin, Phys. Rev. B **84**, 115453 (2011).
[10] A. Bruchhausen, R. Gebs, F. Hudert, D. Issenmann, G. Klatt, A. Bartels, O. Schecker, R. Waitz, A. Erbe, E. Scheer, J. R. Huntzinger, A. Mlayah, and T. Dekorsy, Phys. Rev. Lett. **106**, 077401 (2011).
[11] E. A. Cerda-Mendez, D. N. Krizhanovskii, M. Wouters, R. Bradley, K. Biermann, K. Guda, R. Hey, P. V. Santos, D. Sarkar, and M. S. Skolnick, Phys. Rev. Lett. **105**, 116402 (2010).
[12] D. A. Fuhrmann, S. M. Thon, H. Kim, D. Bouwmeester, P. M. Petroff, A. Wixforth, and H. J. Krenner, Nature Photon. **5**, 605 (2011).
[13] C. Brüggemann, A. V. Akimov, A. V. Scherbakov, M. Bombeck, C. Schneider, S. Hofling, A. Forchel, D. R. Yakovlev, and M. Bayer, Nature Photon. **6**, 30 (2012).
[14] M. Nomura and Y. Arakawa, Nature Photon. **6**, 9 (2012).
[15] V. I. Talyanskii, J. M. Shilton, M. Pepper, C. G. Smith, C. J. B. Ford, E. H. Linfield, D. A. Ritchie, and G. A. C. Jones, Phys. Rev. B **56**, 15 180 (1997).
[16] A. B. Hutchinson, V. I. Talyanskii, M. Pepper, G. Gumbs, G. R. Aĭzin, D. A. Ritchie, and E. H. Linfield, Phys. Rev. B **62**, 6948 (2000).
[17] D. R. Fowler, A. V. Akimov, A. G. Balanov, M. T. Greenaway, M. Henini, T. M. Fromhold, and A. J. Kent, Appl. Phys. Lett. **92**, 232104 (2008).
[18] D. M. Moss, A. V. Akimov, B. A. Glavin, M. Henini, and A. J. Kent, Phys. Rev. Lett. **106**, 066602 (2011).
[19] M. L. Leadbeater, E. S. Alves, F. W. Sheard, L. Eaves, M. Henini, O. H. Hughes, and G. A. Toombs, J. Phys. Condens. Matter **1**, 10 605 (1989).
[20] A. V. Akimov, A. V. Scherbakov, D. R. Yakovlev, C. T. Foxon, and M. Bayer, Phys. Rev. Lett. **97**, 037401 (2006).
[21] G. Tas and H. J. Maris, Phys. Rev. B **49**, 15 046 (1994).
[22] E. Péronne and B. Perrin, Ultrasonics **44**, e1203 (2006).
[23] F. H. Pollak and M. Cardona, Phys. Rev. **172**, 816 (1968).
[24] L. Eaves, M. L. Leadbeater, D. G. Hayes, E. S. Alves, F. W. Sheard, G. A. Toombs, P. E. Simmonds, M. S. Skolnick, M. Henini, and O. H. Hughes, Solid State Electron. **32**, 1101 (1989).
[25] H. Mizuta and T. Tanoue, *The Physics and Applications of Resonant Tunnelling Diodes* (Cambridge University Press, Cambridge, 1995).
[26] A. V. Scherbakov, P. J. S. van Capel, A. V. Akimov, J. I. Dijkhuis, D. R. Yakovlev, T. Berstermann, and M. Bayer, Phys. Rev. Lett. **99**, 057402 (2007).
[27] See Supplemental Material at http://link.aps.org/supplemental/10.1103/PhysRevLett.108.226601 for a detailed analysis of the temporal shape of the strain-induced current pulses, taking into account the reactive circuit elements associated with the RTD and its packaging.